Open-Circuit Fault Diagnosis Based on Deep Learning for Four-Level Active Neutral-Point Clamped Inverters

Dyan Puspita Apsari, Jiwon Jung, and Dong-Choon Lee
Department of Electrical Engineering, Yeungnam University
Gyeongsan, South Korea

***Abstract*—In this paper, a deep learning-based fault diagnosis has been proposed for improving reliability when detect faulty switches of four-level active neutral point clamped (ANPC) inverters. The proposed method detects an open-circuit fault in a single switching device by training a 1-D Convolutional Neural Network (1-D CNN) to extract the periodic feature of pole voltage, which can be done without adding any algorithm for feature extraction. Due to the increased number of switches and conduction paths compared to a two-level inverter, the other method requires complex mathematical equations, threshold settings, and theoretical knowledge of the topology. However, the proposed data-driven deep learning-based method can be made simpler and more robust under different system conditions without using mathematical equations. Simulation results have validated the feasibility of the proposed method that show the diagnostic average accuracy rate reached 99.53 % with conditions that were untrained in the deep learning model.**

***Index Terms*—1D-CNN, deep learning, four-level ANPC inverter, open-circuit fault diagnosis.**

I. Introduction

The multilevel inverters can achieve high efficiency, low output THD, and high performance. Due to these advantages, multilevel inverters have been widely studied for medium-voltage and high-power applications. Various multi-level inverter topologies exist, including Neutral-Point-Clamped Inverters (NPC), Flying-Capacitor Inverters (FCI), and Cascaded H-Bridge Inverters (HBI). Among them, in this paper, a four-level Active Neutral-Point-Clamped (ANPC) Inverter is considered for an open-circuit fault diagnosis [1]. Three-phase four-level ANPC inverters use six active power switches for each phase, this type of inverter is built without a flying capacitor, allowing it to operate over a wide voltage range [2]. However, multilevel inverters are less reliable than two-level inverters due to the larger number of switches, which increases the probability of faults in switching devices. To improve system reliability, the fault diagnosis method of the multilevel inverter has been widely studied. Rapid detection and diagnosis are critical in the operation of multilevel inverters, where open-circuit fault diagnosis methods are particularly important. Due to the potential for further damage to the system, open-switch problems should be detected as soon as possible, whereas short-circuit faults are usually blocked by protection circuits [3].

There are three typical approaches for fault diagnosis, which are the model-based approach, knowledge-based approach, and data-driven approach. Model-based approach needs accurate models, complicated mathematical calculations, and threshold settings [4]. Knowledge-based approach requires extensive knowledge of topology as this approach is based on the analysis of the inverter waveforms and operation in healthy and faulty conditions [5]–[7]. Data driven-based approach data become a crucial part, thus improving data quality and data governance is required. However, theoretical knowledge is not required in this method, and complicated mathematical equations and threshold setting can be avoided [8].

An open-circuit diagnosis technique has been proposed, based on two voltage parameters to detect the faulty switch [7]. Conventional machine learning methods, which are Artificial Neural Networks (ANN), k-Nearest Neighbors (KNN), Support Vector Machines (SVM), and Decision Trees (DT) are used for the diagnosis of a faulty switch [9]–[12]. Furthermore, in the conventional machine learning that mentioned before use specific algorithm for feature extraction, such as Discrete Wavelet Transform (DWT), Fast Fourier Transformation (FFT), and Principal Component Analysis (PCA) [13]–[15]. Feature extraction is a vital step in the dimensionality reduction process by identifying key features in the dataset for the machine learning approach to reduce the number of features. In this work, 1-D time-series data is carried out in the Convolutional Neural Network without the need to apply specific algorithms to select or extract features.

In the fault diagnosis of a four-level ANPC inverter using a data-driven method, data has a large influence on the diagnosis effect, especially under different working conditions. Furthermore, this data-driven method achieves good performance in diagnosis accuracy and robustness. Their computational burden, however, was too high. For this reason, it is important to select the appropriate model and hyperparameter for implementing this data-driven approach. To accomplish a fast diagnosis, a model with low complexity but high accuracy is required. In this paper, 1-D CNN without feature extraction is applied.

II. Open-Circuit Fault Analysis of Four-Level ANPC Inverters

A. Configuration

The representative circuit configuration of a three-phase four-level ANPC inverter topology is shown in Fig. 1. Each phase leg of this inverter, consisting of six active switches, where j represents a phase-leg (a, b, c), and switches such as $S_{1,j}$ and $S_{2,j}$, $S_{3,j}$ and $S_{4,j}$, $S_{5,j}$ and $S_{6,j}$ are complementary switches. This topology shares a common DC-link consisting of three series-connected capacitors. Each capacitor should be maintained at $V_{dc}/3$, which forms the DC link voltage of V_{dc}.

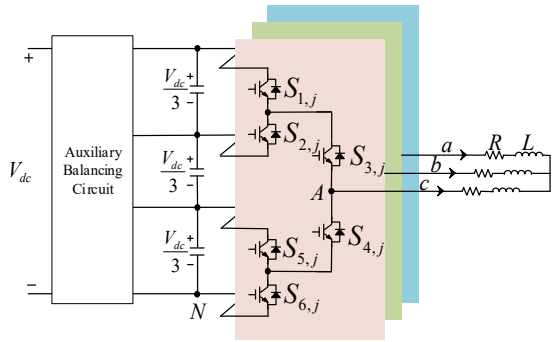

Fig. 1. Three-phase four-level active neutral-point-clamped inverter.

TABLE I
SWITCHING STATES OF 4-LEVEL ACTIVE NEUTRAL-POINT CLAMPED INVERTER

Voltage States	Device Switching States			Pole Voltage
	$S_{1,j}$	$S_{3,j}$	$S_{5,j}$	
V_0	0	0	0	0
V_1	0	0	1	$V_{dc}/3$
V_2	0	1	1	$2V_{dc}/3$
V_3	1	1	1	V_{dc}

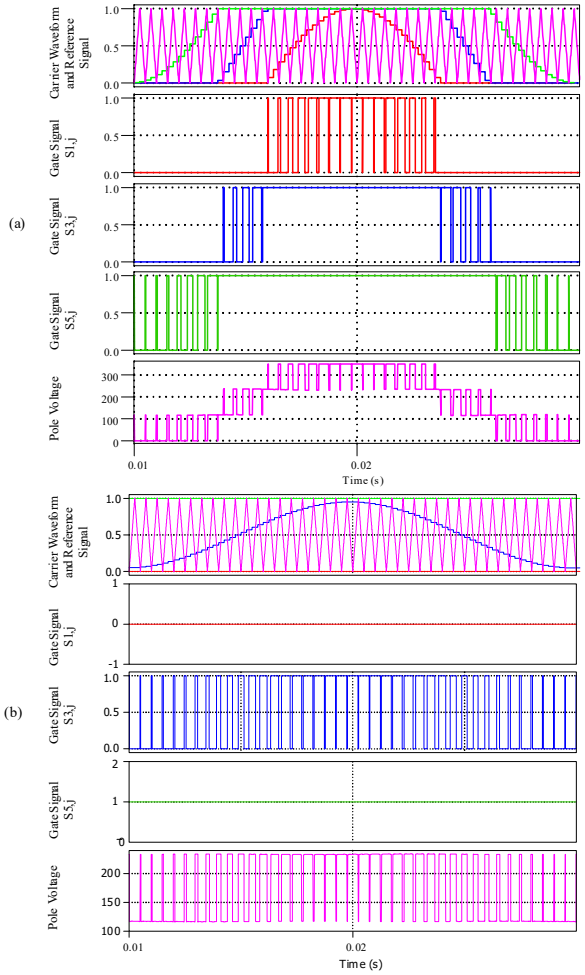

Fig. 2. Level-shifted PWM (LSPWM) for 4L-ANPC inverter operation of (a) m_a = 1.0. (b) m_a = 0.3.

B. Operating Principles and Modulation Method

Operation of four-level ANPC inverter under normal conditions is described in Table I, where the voltage states are determined by switching states of each switch. The switching state 1 and 0 represent ON and OFF states of each switch, respectively.

Fig. 2 shows the level-shifted PWM (LSPWM) applied for the 4L-ANPC inverter [16]. As illustrated in Fig. 2(a), the reference voltage is set for each phase of the 4L-ANPC inverter. The normalized reference voltage is compared with three triangular carrier signals with different levels for one phase, the PWM signal generated by comparing the reference and carrier signals in the previous step is used to turn on and off the IGBTs switch. This topology has limitations due to use LSPWM as modulation method, as can be seen in Fig. 2(a) all six switches are used. Nevertheless, Fig. 2(b) shows a modulation of less than 0.33, it can be seen that not all switches are used. Which is from all of the six switches there are two switches, that is switches $S_{1,j}$ and $S_{6,j}$ for each phase are not used.

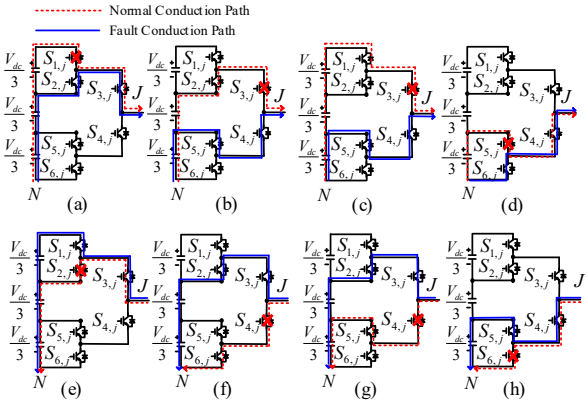

Fig. 3. Open-circuit fault effects on conduction paths in faulty state of (a) $S_{1,j}$ (V_3). (b) $S_{3,j}$ (V_2). (c) $S_{3,j}$ (V_3). (d) $S_{5,j}$ (V_1). (e) $S_{2,j}$ (V_2). (f) $S_{4,j}$ (V_0). (g) $S_{4,j}$ (V_1). (h) $S_{6,j}$ (V_0).

C. Analysis of Open-Circuit Faults

Fig. 3 shows the conduction paths in the cases of open-circuit fault for the 4L-ANPC inverter. If an open-circuit fault occurs at the top switch $S_{1,j}$ as shown in Fig. 3(a), the generation of V_{dc} state is not possible. The $2V_{dc}/3$ and V_{dc} states cannot be generated by the broken 4-L ANPC inverter leg at bridge-side switch $S_{3,j}$, as shown in Fig. 3(b) and (c), respectively. The fault of the lower switch $S_{5,j}$ results in the inability to produce a switching state $V_{dc}/3$, as shown in Fig. 3(d). An open-circuit fault in complementary switches causes the error on the negative side of the output voltage. The waveforms of the output phase voltage are classified into six open-circuit fault cases for single phase, and 18 cases in total for three-phase 4L-ANPC inverters.

The detection of open-circuit fault at $S_{2,j}$ and $S_{5,j}$ take a long time of detection with the conventional method [7]. From the conduction path described in Fig. 3, we can conclude that all possible fault cases have a distinctive effect on the output current. Except for switches $S_{2,j}$ and $S_{5,j}$, which have a combination of faulty switch and output current directions that have no significant effect on the conduction path. Fig. 4 depicts the output current waveform of $S_{2,j}$ and $S_{5,j}$. The two waveforms in Fig. 4(a) and (b) are similar, indicating that these two switches have no significant effect on the output current.

Fig. 3 also shows the effect of the faulty switching state

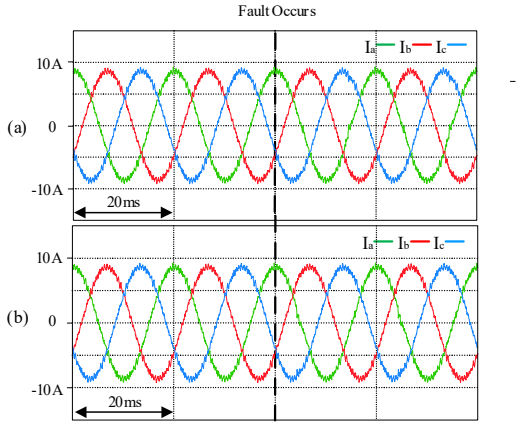

Fig. 4. Waveforms of output currents. (a) Fault at $S_{2,j}$. (b) Fault at $S_{5,j}$.

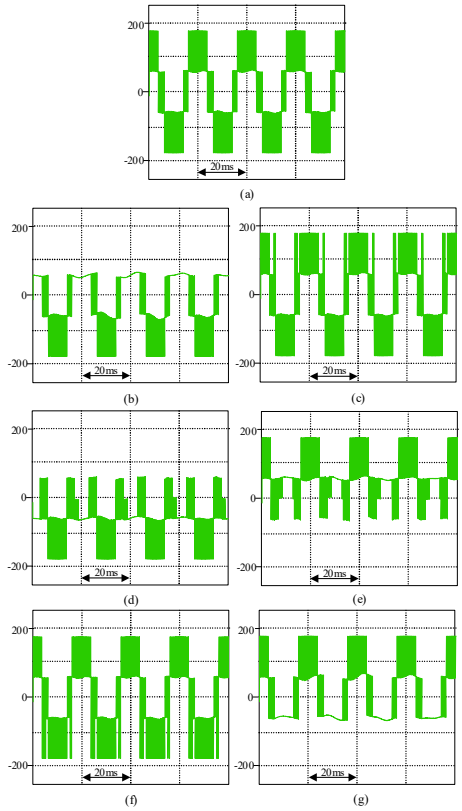

Fig. 5. Waveforms of pole voltages. (a) Normal condition. (b) Fault at $S_{1,j}$. (c) Fault at $S_{2,j}$. (d) Fault at $S_{3,j}$. (e) Fault at $S_{4,j}$. (f) Fault at $S_{5,j}$. (g) Fault at $S_{6,j}$.

on each switch, with each broken switch affecting the formation of each switching state on the 4-level ANPC inverter. Fig. 5 illustrates pole voltage waveforms in the seven cases of open-circuit faults, it can be shown that a faulty switch affects the pole voltage waveform. Previous work [7] used six additional sensors (one inter-half-bridge voltage sensor and one phase voltage sensor per phase) to detect the occurrence of fault. However, using the deep learning approach, the open-circuit fault can be diagnosis with three additional pole voltage sensors. In this work, the two schemes of input are compared to show that even when using fewer input data open-circuit fault diagnosis in a 4L-ANPC inverter classification can be identified correctly. The first scheme utilizes six inputs which consist

TABLE II
SIMULATION CONDITION

Parameters	Values
Switching frequency	f_{sw} = 2000 Hz
DC-link voltage	V_{dc} = 350 V
Load	R = 20 Ω, L = 6 mH

of three output currents and three pole voltages (I_a, I_b, I_c, V_{AN}, V_{BN}, V_{CN}). The second scheme uses three inputs, which are only using three pole voltages (V_{AN}, V_{BN}, V_{CN}).

III. 1-D CNN-Based Fault Diagnosis Method

A. Data Acquisition

As mentioned in the previous section, the distorted pole voltage can be used to pinpoint the location of the open circuit fault in the 4L-ANPC inverter. The conventional method requires a deep understanding of the topology, and the computation time for each diagnosis is also a disadvantage of this method. Deep learning is a data-driven learning approach that extracts regularity and features from a large set of data. Deep learning is capable of self-learning, error-tolerance, complex pattern recognition, and make fast diagnosis. In this work, 1-D CNN is used for faulty switch diagnosis, while PLECS simulations are used for data acquisition. Table II shows the simulation conditions used to collect training and validation data. Three-pole voltages are considered as the input data of fault information, for which one pole voltage sensor for each phase is installed to acquire raw data. With a sampling frequency of 10 kHz, a waveform with a two-cycle length of a fundamental frequency is extracted by taking into consideration all three phases with a size of 3x200.

The training dataset includes three-phase pole voltage data under three fundamental frequencies (10 Hz, 20 Hz, and 50 Hz) and four modulation indexes (0.2, 0.5, 0.8, and 1.0). Several factors are considered when determining the training dataset. Firstly, three fundamental frequencies for training data is used because low fundamental frequency requires more input size for each cycle than high fundamental frequency. For this reason, data training in low fundamental frequency is required to achieve high-accuracy performance. Secondly, the use of four modulation indexes in data training is due to the limitations of LSPWM mentioned above. As a result, data training at low modulation index is required, and the two switches stated above are not employed for input data. Every fundamental frequency dataset contains four modulation indexes for each of the 19 cases of faulty switches. The amount of data used in each fundamental frequency is as follows: 54,872 samples for 10 Hz data, 45,080 samples for 20 Hz data, and 28,700 samples for 50 Hz data.

In this work, two methods are used to collect large amounts of data while avoiding data duplication. Firstly, in the CNN model training process. If a large amount of 1-D time-series data is fed into the CNN model at once, this might affect computer memory, which will require a larger memory for larger input data. To divide the long 1-D time-series data into short data segments and to improve the generalization ability and robustness of the trained CNN model, data segmentation is applied in the model. Using

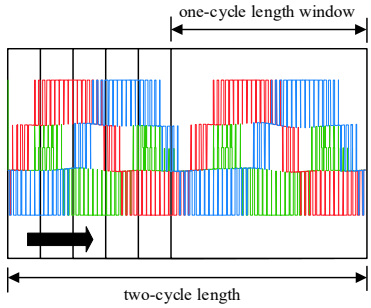

Fig. 6. Data segmentation using window slicing.

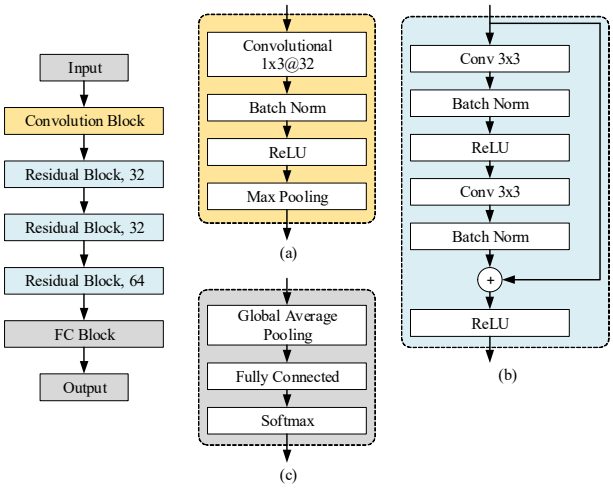

Fig. 7. 1D-CNN model structure.

data segmentation, the two-cycle length of waveform data is window-sliced with one-cycle-length window and divided while keeping the periodic features. Furthermore, the window slicing method allows ignorance of the data starting point in periodic data. Fig. 6 shows the process of data segmentation using window slicing. Secondly, data is extracted to consider the transient condition after causing a fault at every 1/5 of the cycle. In the data acquisition process, input data of 1-D CNN often has a variety of magnitudes and amplitudes. To solve the problem of not being able to train every magnitude, avoid losing the polarity of the data, avoid local optimization, and be unaffected by voltage amplitude, normalization is performed as data preprocessing from -1 to 1.

B. 1-D CNN Model Structure

As mentioned previously, different CNN model structures and hyperparameters may produce different results. Selecting the appropriate model structure and hyperparameters can significantly improve fault diagnosis performance. Fig. 7 depicts the detailed 1-D CNN model structure of the proposed fault diagnosis algorithm, which consists of a convolution block, a residual block, and a fully connected block. In the figure, the numbers 32, 32, and 64 represent the number of convolution channels. As shown in Fig. 7(a), the convolution block consists of a convolutions layer and a max pooling layer. As a result, the output feature map of the convolution block is of a half the size of the input with 32 channels. Fig. 7(b) depicts three residual blocks, each of which stacked two conv3x3

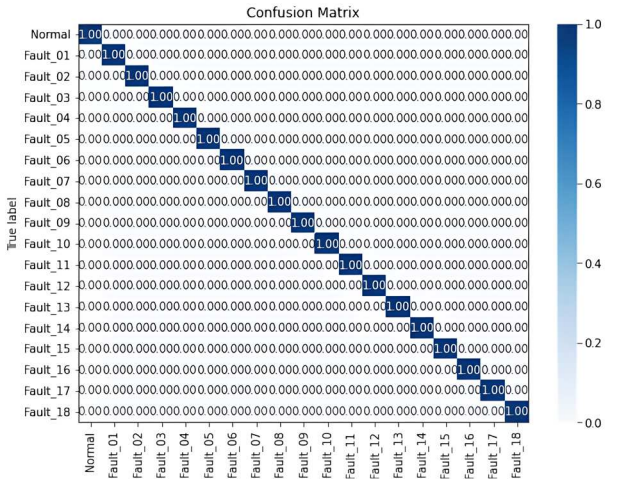

Fig. 8. Confusion matrix of training result.

identity mappings, allowing us to explore more of the raw data's feature space. The conv 3x3 layer refers to the convolution layers that use a 3 x 3 kernel size. As shown in Fig. 7(c), the fully connected block of the model uses a Global Average Pooling layer (GAP) and a Fully Connected layer (FCL). Finally, the SoftMax activation function is used to determine the probability of recurrence in 19 fault cases.

C. Training 1-D CNN Model

In this research, three-pole voltage data are considered as input data. Simulation data for one normal case and 18 fault cases are extracted, giving 19 fault cases with 128,652 samples that will be included in the 1-D CNN model. The input dataset is randomly divided into two groups, with a ratio of 85 % utilized as the training set and 15 % utilized as the validation set to generate the training dataset samples of 109,354 and 19,298, respectively. While training a 1-D CNN model, Adam is used to optimizing the model, whereas cross-entropy loss is employed as the loss function for training in multiclass classification. In this paper, the number of samples in each batch and epoch is set as 300 and 30, respectively. Fig. 8 shows that the proposed networks perform well on the training dataset which achieves 100 % accuracy.

IV. Performance Evaluation

A. Validation Result

In this work, the feasibility of the open-circuit fault diagnosis using the deep learning approach is verified by simulation. The validation data are generated by one normal operation and 18 faulty operations. Using 1D-Convolutional Neural Network (1D-CNN) models, the proposed method utilizes three-pole voltage signals as an important characteristic to classify fault conditions. The proposed system is tested on data sets created under various situations following the acquisition and simulation conditions. Since any changes in modulation index and fundamental frequency affect pole voltages, the system should detect and identify each switch fault regardless of modulation index and fundamental frequency to provide a reliable application.

TABLE III
CLASSIFICATION ACCURACY OF DIFFERENT FUNDAMENTAL FREQUENCIES FOR DIFFERENT MODULATION INDEX

Fundamental frequency	Modulation index							
	Six inputs				Three inputs			
	0.1	0.4	0.7	0.9	0.1	0.4	0.7	0.9
10 Hz	98.21 %	97.56 %	98.81 %	98.75 %	99.16 %	97.22 %	98.89 %	98.43 %
20 Hz	99.59 %	100 %	100 %	100 %	100 %	100 %	100 %	100 %
50 Hz	100 %	99.07 %	100 %	99.95 %	100 %	100 %	100 %	100 %
60 Hz	100 %	100 %	99.76 %	99.56 %	100 %	99.51 %	99.27 %	100 %

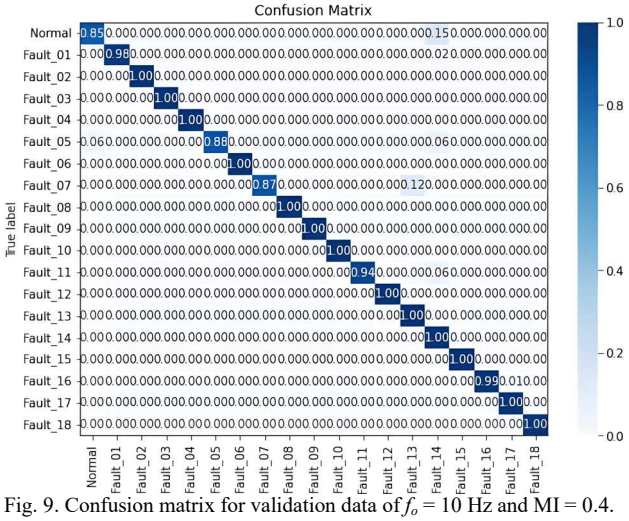

Fig. 9. Confusion matrix for validation data of f_o = 10 Hz and MI = 0.4.

Validation datasets are simulated by changing four fundamental frequencies (10 Hz, 20 Hz, 50 Hz, and 60 Hz) and four modulation indexes (0.1, 0.4, 0.7, and 0.9). These system conditions for validation are used because there is less information at low fundamental frequency than at high fundamental frequency, so the lower fundamental frequency is used as validation data to validate the model. Another condition is that a low modulation index can produce a different pole voltage waveform than a high modulation index. When utilizing LSPWM as the modulation technique, 0.3 has a different waveform than 0.6, as previously mentioned, $S_{1,j}$ and $S_{6,j}$ for each phase are not used for modulation less than 0.33. The accuracy is reduced when the fundamental frequency is low. This is because higher fundamental frequencies provide more information in the same input size as lower fundamental frequencies. Table III lists the classification accuracy result of the validation dataset from an untrained dataset. As can be seen, the proposed networks perform well using RL load (R = 20 Ω and L = 6 mH) with the average accuracy rate of the model on the validation dataset reaching 99.53 %, illustrating the reliability that can achieve high accuracies of different fundamental frequency for different modulation index. Table III also shows that even though the input is changed, the accuracy does not change significantly. This shows that open-circuit fault diagnosis in a 4L-ANPC inverter can be identified correctly even with only three inputs data (three-pole voltages).

B. Performance Evaluation of Fault Diagnosis

The performance of model classification can be assessed in terms of the most common metrics. In the performance evaluation of classification, sensitivity,

TABLE IV
THE EVALUATION RESULT FOR VALIDATION DATA OF F_O = 10HZ AND MI = 0.4

Cases	Precision rate	Recall rate	F1-score	Sample
Normal	0.94	0.85	0.89	410
Fault 1	1.00	0.98	0.99	410
Fault 2	1.00	1.00	1.00	410
Fault 3	1.00	1.00	1.00	410
Fault 4	1.00	1.00	1.00	410
Fault 5	1.00	0.88	0.94	410
Fault 6	1.00	1.00	1.00	410
Fault 7	1.00	0.87	0.93	410
Fault 8	1.00	1.00	1.00	410
Fault 9	1.00	1.00	1.00	410
Fault 10	1.00	1.00	1.00	410
Fault 11	0.99	0.94	0.96	410
Fault 12	1.00	1.00	1.00	410
Fault 13	0.81	1.00	0.90	410
Fault 14	0.77	1.00	0.87	410
Fault 15	1.00	1.00	1.00	410
Fault 16	1.00	0.99	1.00	410
Fault 17	0.97	1.00	0.99	410
Fault 18	1.00	1.00	1.00	410
Average/Total	0.97	0.97	0.97	7790

precision, and F1-score are widely used. These standard performance metrics are calculated using the true positive (TP), true negative (TN), false positive (FP), and false negative (FN) [17].

The definition of each metric is defined as: Accuracy refers to the ratio of correctly classified fault to the total result, Precision is the ratio of correctly classified fault cases out of the total predicted fault result, Sensitivity (Recall) rate refers to the ratio of correct fault case that was classified, and F1-measure refers to the combined Precision and Recall obtaining a balanced classification model. A good model needs to balance between Precision and Recall. These metrics are calculated according to equations (1)-(4) [18]:

$$Accuracy = \frac{TP + TN}{TP + TN + FP + FN} \tag{1}$$

$$Precision = \frac{TP}{TP + FP} \tag{2}$$

$$Recall = \frac{TP}{TP + FN} \tag{3}$$

$$F1 - Score = \frac{2 * Precision * Recall}{(Precision + Recall)} \tag{4}$$

Fig. 9 shows the confusion matrix and Table IV lists evaluation results at f_o = 10Hz and MI = 0.4. These data

conclude in the least accurate result of 97.22 %. As can be seen in Fig. 9, normal operation has the lowest accuracy of 85 %, with 62 samples misclassified as fault 14. This misclassified data results in low accuracy, and inaccurate classification problems can be identified using the confusion matrix data. The main reason for the low accuracy in this validation data is insufficient or poor-quality data for training the model. This may occur if the dataset is too small or biased. In certain circumstances, the model may lack sufficient information to learn from, or it may be learning from irrelevant data, resulting in low accuracy.

The precision/recall trade-off is listed in Table IV. Fault 14 has the lowest precision rate (77 %) and F1 score (87 %), whereas the normal case has the lowest recall rate (85 %). A model can have high accuracy but a low recall since it fails to predict several classes. On the other hand, the models with higher recall but lower accuracy will result in more inaccurate fault identification classifications. As can be seen, recall is critical to reducing the possibility of missing positive cases. In many circumstances, missing a positive case has a considerably higher cost than incorrectly labeling something as positive. However, the comprehensive results verify that the proposed method can effectively diagnose various fundamental frequency for various modulation index.

V. Conclusions

This paper proposed an open-circuit fault diagnosis method for a 4L-ANPC inverter, based on 1-D CNN. The conventional fault diagnosis method relies on the extensive knowledge of multilevel inverter, and it is difficult to identify the faults of two switches, which are $S_{2,j}$ or $S_{5,j}$ of each phase. The 1-D CNN model formed of three blocks consists of a convolution block, a residual block, and a fully connected block for classification. The proposed method can do the feature extraction from 1-D time-series data without any signal processing operations. To improve the performance, the dataset of pole voltages by using the window slicing method is normalized between -1 and 1. For the deep learning model, data training 30 times was carried out using Adam. The proposed method was validated with simulation results that show the diagnostic average accuracy rate reached 99.53 % with conditions that were untrained in the deep learning model. Using classification performance evaluation, it is possible to conclude that the proposed method can perform with high accuracy across a wide range of operations while requiring fewer input data.

Acknowledgment

This work was supported by the National Research Foundation of Korea (NRF) grant funded by the Korea government (MSIT) (No. 2022R1A4A1031885)

References

[1] S. Yang, A. Bryant, P. Mawby, D. Xiang, L. Ran, and P. Tavner, "An industry-based survey of reliability in power electronic converters," *IEEE Trans. Ind. Appl.*, vol. 47, no. 3, pp. 1441–1451, 2011.

[2] K. Wang, Z. Zheng, and Y. Li, "Topology and control of a four-level ANPC inverter," *IEEE Trans. Power Electron.*, vol. 35, no. 3, pp. 2342–2352, 2020.

[3] B. Lu and S. K. Sharma, "A literature review of IGBT fault diagnostic and protection methods for power inverters," *IEEE Trans. Ind. Appl.*, vol. 45, no. 5, pp. 1770–1777, 2009.

[4] M. A. Mazzoletti, G. R. Bossio, C. H. De Angelo, and D. R. Espinoza-Trejo, "A model-based strategy for interturn short-circuit fault diagnosis in PMSM," *IEEE Trans. Ind. Electron.*, vol. 64, no. 9, pp. 7218–7228, 2017.

[5] X. Pei, S. Nie, Y. Chen, and Y. Kang, "Open-circuit fault diagnosis and fault-tolerant strategies for full-bridge DC-DC converters," *IEEE Trans. Power Electron.*, vol. 27, no. 5, pp. 2550–2565, 2012.

[6] R. Peuget, S. Courtine, and J. P. Rognon, "Fault detection and isolation on a PWM inverter by knowledge-based model," *IEEE Trans. Ind. Appl.*, vol. 34, no. 6, pp. 1318–1326, 1998.

[7] J. Pribadi and D. C. Lee, "Open-switch fault diagnosis in four-level active neutral-point-clamped inverter," *Proc. 2021 IEEE ECCE*, pp. 2576–2581, 2021.

[8] W. Gong, H. Chen, Z. Zhang, M. Zhang, and H. Gao, "A data-driven-based fault diagnosis approach for electrical power DC-DC inverter by using modified convolutional neural network with global average pooling and 2-D feature image," *IEEE Access*, vol. 8, pp. 73677–73697, 2020.

[9] S. Khomfoi and L. M. Tolbert, "Fault diagnostic system for a multilevel inverter using a neural network," *IEEE Trans. Power Electron.*, vol. 22, no. 3, pp. 1062–1069, 2007.

[10] Q. P. He and J. Wang, "Fault detection using the k-nearest neighbor rule for semiconductor manufacturing processes," *IEEE Trans. Semicond. Manuf.*, vol. 20, no. 4, pp. 345–354, 2007.

[11] I. Bandyopadhyay, P. Purkait, and C. Koley, "Performance of a classifier based on time-domain features for incipient fault detection in inverter drives," *IEEE Trans. Ind. Informatics*, vol. 15, no. 1, pp. 3–14, 2019.

[12] A. R. Mohammed, S. A. Mohammed, D. Cote, and S. Shirmohammadi, "Machine learning-based network status detection and fault localization," *IEEE Trans. Instrum. Meas.*, vol. 70, no. 16892594, 2021.

[13] Y. Y. Hong and M. T. A. M. Cabatac, "Fault detection, classification, and location by static switch in microgrids using wavelet transform and taguchi-based artificial neural network," *IEEE Syst. J.*, vol. 14, no. 2, pp. 2725–2735, 2020.

[14] B. Cai, Y. Zhao, H. Liu, and M. Xie, "A data-driven fault diagnosis methodology in three-phase inverters for PMSM drive systems," *IEEE Trans. Power Electron.*, vol. 32, no. 7, pp. 5590–5600, 2017.

[15] S. Khomfoi and L. M. Tolbert, "Fault diagnosis and reconfiguration for multilevel inverter drive using AI-based techniques," *IEEE Trans. Ind. Electron.*, vol. 54, no. 6, pp. 2954–2968, 2007.

[16] H. R. Nielsen, "Us 7.688,048 B2," vol. 2, no. 12, pp. 1–4, 2010.

[17] C. Yin, Y. Zhu, J. Fei, and X. He, "A deep learning approach for intrusion detection using recurrent neural networks," *IEEE Access*, vol. 5, pp. 21954–21961, 2017.

[18] J. G. Choi, I. Ko, J. Kim, Y. Jeon, and S. Han, "Machine learning framework for multi-level classification of company revenue," *IEEE Access*, vol. 9, pp. 96739–96750, 2021.